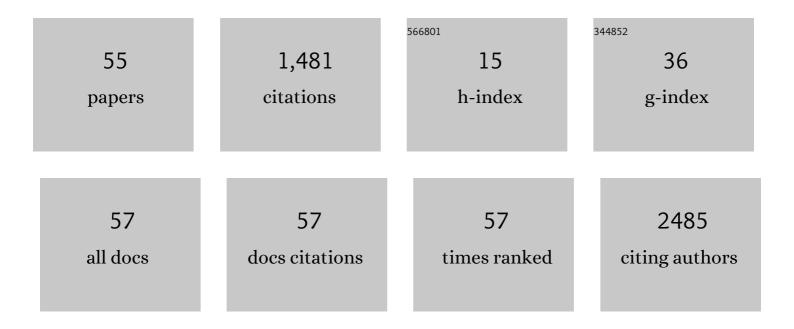
Meng-Su Zeng

List of Publications by Year in descending order

Source: https://exaly.com/author-pdf/1897191/publications.pdf Version: 2024-02-01



MENC-SU ZENC

#	Article	IF	CITATIONS
1	Guidelines for Diagnosis and Treatment of Primary Liver Cancer in China (2017 Edition). Liver Cancer, 2018, 7, 235-260.	4.2	426
2	Efficacy of Berberine in Patients with Non-Alcoholic Fatty Liver Disease. PLoS ONE, 2015, 10, e0134172.	1.1	163
3	Assessment of Microvascular Invasion of Hepatocellular Carcinoma with Diffusion Kurtosis Imaging. Radiology, 2018, 286, 571-580.	3.6	123
4	CT texture analysis in colorectal liver metastases: A better way than size and volume measurements to assess response to chemotherapy?. United European Gastroenterology Journal, 2016, 4, 257-263.	1.6	99
5	Wholeâ€liver CT texture analysis in colorectal cancer: Does the presence of liver metastases affect the texture of the remaining liver?. United European Gastroenterology Journal, 2014, 2, 530-538.	1.6	56
6	Pneumomediastinum and pneumoperitoneum on computed tomography after peroral endoscopic myotomy (POEM): postoperative changes or complications?. Acta Radiologica, 2015, 56, 1216-1221.	0.5	53
7	Wholeâ€ŧumor MRI histogram analyses of hepatocellular carcinoma: Correlations with Kiâ€67 labeling index. Journal of Magnetic Resonance Imaging, 2017, 46, 383-392.	1.9	49
8	MRI of small intrahepatic mass-forming cholangiocarcinoma and atypical small hepatocellular carcinoma (â‰8 cm) with cirrhosis and chronic viral hepatitis: a comparative study. Clinical Imaging, 2014, 38, 265-272.	0.8	29
9	Different MR features for differentiation of intrahepatic mass-forming cholangiocarcinoma from hepatocellular carcinoma according to tumor size. British Journal of Radiology, 2018, 91, 20180017.	1.0	27
10	Single-breath-hold T2WI liver MRI with deep learning-based reconstruction: A clinical feasibility study in comparison to conventional multi-breath-hold T2WI liver MRI. Magnetic Resonance Imaging, 2021, 81, 75-81.	1.0	27
11	Pre-TACE kurtosis of ADCtotal derived from histogram analysis for diffusion-weighted imaging is the best independent predictor of prognosis in hepatocellular carcinoma. European Radiology, 2019, 29, 213-223.	2.3	22
12	Magnetic resonance texture analysis for the identification of cytokeratin 19-positive hepatocellular carcinoma. European Journal of Radiology, 2019, 117, 164-170.	1.2	22
13	Performance comparison between MRI and CT for local staging of sigmoid and descending colon cancer. European Journal of Radiology, 2019, 121, 108741.	1.2	22
14	Pre-treatment ADC image-based random forest classifier for identifying resistant rectal adenocarcinoma to neoadjuvant chemoradiotherapy. International Journal of Colorectal Disease, 2020, 35, 101-107.	1.0	22
15	Gd-EOB-DTPA-enhanced magnetic resonance imaging for focal liver lesions in Chinese patients: a multicenter, open-label, phase III study. Hepatobiliary and Pancreatic Diseases International, 2013, 12, 607-616.	0.6	17
16	Histogram Analysis of Diffusion Kurtosis Magnetic Resonance Imaging for Diagnosis of Hepatic Fibrosis. Korean Journal of Radiology, 2018, 19, 916.	1.5	16
17	Assessing liver fibrosis in chronic hepatitis B using MR extracellular volume measurements: Comparison with serum fibrosis indices. Magnetic Resonance Imaging, 2019, 59, 39-45.	1.0	16
18	MR features based on LI-RADS identify cytokeratin 19 status of hepatocellular carcinomas. European Journal of Radiology, 2019, 113, 7-14.	1.2	16

Meng-Su Zeng

#	Article	IF	CITATIONS
19	Analysis of m6A-Related IncRNAs for Prognosis Value and Response to Immune Checkpoint Inhibitors Therapy in Hepatocellular Carcinoma. Cancer Management and Research, 2021, Volume 13, 6451-6471.	0.9	16
20	Novel Imaging Diagnosis for Hepatocellular Carcinoma: Consensus from the 5th Asia-Pacific Primary Liver Cancer Expert Meeting (APPLE 2014). Liver Cancer, 2015, 4, 215-227.	4.2	14
21	Difference analysis in prevalence of incidental pancreatic cystic lesions between computed tomography and magnetic resonance imaging. BMC Medical Imaging, 2019, 19, 43.	1.4	14
22	T 1 mapping on gadoxetic acid-enhanced MR imaging predicts recurrence of hepatocellular carcinoma after hepatectomy. European Journal of Radiology, 2018, 103, 25-31.	1.2	13
23	Usefulness of two-point Dixon fat-water separation technique in gadoxetic acid-enhanced liver magnetic resonance imaging. World Journal of Gastroenterology, 2015, 21, 5017.	1.4	13
24	Microvascular invasion of small hepatocellular carcinoma can be preoperatively predicted by the 3D quantification of MRI. European Radiology, 2022, 32, 4198-4209.	2.3	13
25	Preoperative evaluation of colorectal liver metastases: comparison of gadopentetate dimeglumine and gadoxetic-acid-enhanced 1.5-T MRI. Clinical Imaging, 2014, 38, 273-278.	0.8	12
26	CT-detected extramural venous invasion is corelated with presence of lymph node metastasis and progression-free survival in gastric cancer. British Journal of Radiology, 2020, 93, 20200673.	1.0	12
27	Skewness of apparent diffusion coefficient (ADC) histogram helps predict the invasive potential of intraductal papillary neoplasms of the bile ducts (IPNBs). Abdominal Radiology, 2019, 44, 95-103.	1.0	11
28	Impact of visceral adipose tissue on the accuracy of T-staging by CT in colon cancer. European Journal of Radiology, 2021, 134, 109400.	1.2	10
29	Identifying response in colorectal liver metastases treated with bevacizumab: development of RECIST by combining contrast-enhanced and diffusion-weighted MRI. European Radiology, 2021, 31, 5640-5649.	2.3	10
30	Comprehensive analysis of tumor immune microenvironment and prognosis of m6A-related lncRNAs in gastric cancer. BMC Cancer, 2022, 22, 316.	1.1	10
31	Crosstalk Between Metabolism and Immune Activity Reveals Four Subtypes With Therapeutic Implications in Clear Cell Renal Cell Carcinoma. Frontiers in Immunology, 2022, 13, 861328.	2.2	10
32	Role of MR in the differentiation of IgG4-related from non-IgG4-related hepatic inflammatory pseudotumor. Hepatobiliary and Pancreatic Diseases International, 2017, 16, 631-637.	0.6	9
33	A multidimensional nomogram combining imaging features and clinical factors to predict the invasiveness and metastasis of combined hepatocellular cholangiocarcinoma. Annals of Translational Medicine, 2021, 9, 1518-1518.	0.7	9
34	Detection of Endogenous Iron Reduction during Hepatocarcinogenesis at Susceptibility-Weighted MR Imaging: Value for Characterization of Hepatocellular Carcinoma and Dysplastic Nodule in Cirrhotic Liver. PLoS ONE, 2015, 10, e0142882.	1.1	9
35	Combined arterial and delayed enhancement patterns of MRI assist in prognostic prediction for intrahepatic mass-forming cholangiocarcinoma (IMCC). Abdominal Radiology, 2022, 47, 640-650.	1.0	9
36	Myocardial extracellular volume fraction measurement in chronic total coronary occlusion: Association with myocardial injury, angiographic collateral flow, and functional recovery. Journal of Magnetic Resonance Imaging, 2016, 44, 972-982.	1.9	8

Meng-Su Zeng

#	Article	IF	CITATIONS
37	Left Ventricular Outflow Tract Obstruction in Hypertrophic Cardiomyopathy: The Utility of Myocardial Strain Based on Cardiac <scp>MR</scp> Tissue Tracking. Journal of Magnetic Resonance Imaging, 2021, 53, 51-60.	1.9	8
38	Hepatocellular carcinoma 20Âmm or smaller in cirrhosis patients: early magnetic resonance enhancement by gadoxetic acid compared with gadopentetate dimeglumine. Hepatology International, 2014, 8, 104-111.	1.9	7
39	Histogram analyses of diffusion kurtosis indices and apparent diffusion coefficient in assessing liver regeneration after ALPPS and a comparative study with portal vein ligation. Journal of Magnetic Resonance Imaging, 2018, 47, 729-736.	1.9	7
40	Feasibility of compressed sensing technique for isotropic dynamic contrast-enhanced liver magnetic resonance imaging. European Journal of Radiology, 2021, 139, 109729.	1.2	7
41	Assessment of liver regeneration after associating liver partition and portal vein ligation for staged hepatectomy: a comparative study with portal vein ligation. Hpb, 2018, 20, 305-312.	0.1	6
42	Applying Nitroglycerin at Coronary MR Angiography at 1.5 T: Diagnostic Performance of Coronary Vasodilation in Patients with Coronary Artery Disease. Radiology: Cardiothoracic Imaging, 2020, 2, e190018.	0.9	6
43	Risk stratification of LI-RADS M and LI-RADS 4/5 combined hepatocellular cholangiocarcinoma: prognostic values of MR imaging features and clinicopathological factors. European Radiology, 2022, 32, 5166-5178.	2.3	6
44	The diagnosis of coronary plaque stability by multi-slice computed tomography coronary angiography. Journal of Thoracic Disease, 2018, 10, 2365-2376.	0.6	5
45	The prognostic value of global myocardium strain by CMR-feature tracking in immune checkpoint inhibitor–associated myocarditis. European Radiology, 2022, 32, 7657-7667.	2.3	5
46	Magnetic resonance morphologic features predict progression of incidental pancreatic cystic lesions during follow-up. Diagnostic and Interventional Radiology, 2020, 26, 396-402.	0.7	4
47	Utility of preoperative computed tomography features in predicting the Ki-67 labeling index of gastric gastrointestinal stromal tumors. European Journal of Radiology, 2021, 142, 109840.	1.2	4
48	Unenhanced Whole-Heart Coronary MRA: Prospective Intraindividual Comparison of 1.5-T SSFP and 3-T Dixon Water-Fat Separation GRE Methods Using Coronary Angiography as Reference. American Journal of Roentgenology, 2022, 219, 199-211.	1.0	3
49	Hepatobiliary phase images of gadoxetic acid-enhanced MRI may improve accuracy of predicting the size of hepatocellular carcinoma at pathology. Acta Radiologica, 2022, 63, 734-742.	0.5	2
50	Coronary CT Angiography in Asymptomatic Adults with Hepatic Steatosis. Radiology, 2021, 301, 593-601.	3.6	2
51	Assessment of the acute effects of glucocorticoid treatment on coronary microembolization using cine, first-pass perfusion, and delayed enhancement MRI. Journal of Magnetic Resonance Imaging, 2016, 43, 921-928.	1.9	1
52	Three-Dimensional Free-Breathing Whole-Heart Coronary Magnetic Resonance Angiography at 1.5 T. Journal of Computer Assisted Tomography, 2019, 43, 919-925.	0.5	1
53	Visualizing Central Vessels of Hepatic Angiomyolipoma Devoid of Fat Using a 2D Multi-Breath-Hold Susceptibility-Weighted Imaging. Case Reports in Radiology, 2015, 2015, 1-5.	0.5	0
54	Value of whole-liver apparent diffusion coefficient histogram analysis for quantification of liver fibrosis stages. Chinese Journal of Academic Radiology, 2019, 1, 6-12.	0.4	0

#	Article	IF	CITATIONS
55	MR dynamic Gadolinium-enhanced fast multiplanar spoiled gradient-echo and spin-echo T1-weighted fat-suppressed techniques in diagnosis of pancreatic carcinoma. Hepatobiliary and Pancreatic Diseases International, 2002, 1, 294-8.	0.6	0